Advanced Synthesis & Catalysis

Accepted Article

Title: Quantitative Prediction of Yield in Transglycosylation Reaction Catalyzed by Nucleoside Phosphorylases

Authors: Cyril Alexeev, Irina V. Kulikova, Sergei Gavryushov, Vitali I. Tararov, and Sergey Mikhailov

To be cited as: *Adv. Synth. Catal.* 10.1002/adsc.201800411

Link to VoR: http://dx.doi.org/10.1002/adsc.201800411

10.1002/adsc.201800411

FULL PAPER

DOI: 10.1002/adsc.201((will be filled in by the editorial staff))

Quantitative Prediction of Yield in Transglycosylation Reaction Catalyzed by Nucleoside Phosphorylases

Cyril S. Alexeev[a], Irina V. Kulikova[a], Sergei Gavryushov[a,b], Vitali I. Tararov[a] und Sergey N. Mikhailov[a]*

[a] Engelhardt Institute of Molecular Biology, Russian Academy of Sciences, Vavilov str. 32, 119991 Moscow, Russia [*Correspondance to smikh@eimb.ru, tel. +7-499-135-9733]

[b] Sechenov First Moscow State Medical University, 2-4 Bolshaya Pirogovskaya st., Moscow 119991, Russia

Received: ((will be filled in by the editorial staff))

Supporting information for this article is available on the WWW under http://dx.doi.org/10.1002/adsc.201######.((Please delete if not appropriate))

Abstract. Phosphorolytic transglycosylation catalyzed by nucleoside phosphorylases is an important biotechnological process. The reaction is reversible, and the yield of the target nucleoside depends on its concentration at the equilibrium state. We have shown that initial concentrations of the starting compounds and the phosphorolysis equilibrium constants of starting and final glycosides determine concentrations of all the components at the equilibrium state. Based on that, we developed a novel quantitative approach for the prediction of yields in transglycosylation reactions. This method simplifies the choice of reagent concentrations and their ratios for the maximization of the target nucleoside yield. It is advantageous over widely applied blind and cumbersome trial-and-error approach and can reduce the required chemical and energy resources. The described algorithm could also be applied for other equilibrium transfer reactions.

Keywords: nucleoside phosphorolysis; nucleoside phosphorylases; transglycosylation; equilibrium constants; prediction and maximization of reaction outcome

Introduction

Nucleoside analogues form an important class of biologically active compounds. Currently more than dozen of them are used in the antitumor or antiviral therapy.[1] In addition, the use of nucleoside analogs as potential antibiotics [2] and radiopharmaceuticals [3] has recently been reported. The importance of these compounds in medicine elucidates permanent interest in elaboration of efficient methods of their synthesis.

The vast majority of nucleoside analogs is prepared by chemical synthetic methods. There are two main approaches: modification of the available nucleoside (exemplified in ref. [4]), and coupling of the nucleic base with monosaccharide, which is most common. Both approaches are multi-step and time-consuming chemical procedures. They require a variety of reagents and organic solvents, the usage of orthogonal protective groups, include several protection/deprotection steps and activating of appropriate positions of reacting molecules. A challenging problem is the stereocontrolled formation of the glycosydic bond. Although this problem was successfully solved with ribose derivatives, the use of 2′-deoxyribose results in the formation of a mixture of α- and β-anomers.[5] In contrast to that, enzymatically catalyzed glycosylation of nucleobases is a stereospecific one-step reaction, which is carried out in an aqueous solution.

Nucleoside phosphorylases (NPs) catalyze phosphorolytic cleavage of (deoxy)nucleosides (rB1) with the formation of α-D-(2-deoxy)ribose-1-phosphate (rP) and corresponding nucleobase (B1) (Phosphorolysis, Scheme 1).[6] This reaction is reversible, and the equilibrium of the reaction is shifted towards nucleosides.[7] The process opposite to phosphorolysis is the nucleoside synthesis. For the preparation of nucleosides ribosophosphate analogs (rP) are usually used.[1]

Because of high price of pentose-1-phosphates (rP), the alternative method of enzymatic transglycosylation (Scheme 1) was suggested. It consists in a transfer of the carbohydrate residue from one heterocyclic base B1 to another B2 via parent ribosophosphate (rP) formation. Depending on the used NPs, this process results in the formation of the new nucleoside (rB2). This approach is actively

developed and applied for the synthesis of practically important nucleosides.[8] Among applications of this method, synthesis of natural[8] as well as synthetic (cladribine,[9] 5-substituted 2'-deoxyribopyrimidines [10]) nucleosides should be mentioned. In this type of reactions, uridine (or thymidine) and purine nucleoside phosphorylases are used for transfer of both natural and synthetic nucleosides.

Originally, the term transglycosylation arises from carbohydrate chemistry meaning the enzymatic transfer of sugar from oligosaccharide to another carbohydrate acceptor.[11] Such non-phosphorolytic transglycosylation can be achieved with 2′-deoxyribosyltransferase[12] and nucleoside hydrolase.[13]

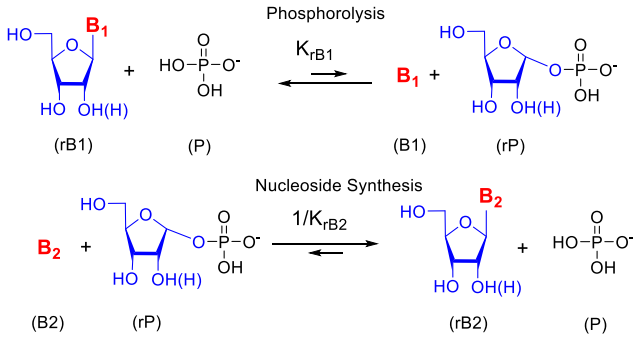

$$K_{rB1} = \frac{[rP][B1]}{[rB1][P]}, \quad K_{rB2} = \frac{[rP][B2]}{[rB2][P]}$$

Scheme 1. General scheme of reversible transglycosylation reaction.

For the successful application of phosphorolytic transglycosylation in the synthesis of target nucleosides, it is necessary to have theoretical understanding of the process. Unfortunately, it has remained undeveloped until now, though the process is widely applied. Only some intuitive hints on the interplay of phosphorolysis equilibrium constants (K_{rB1} and K_{rB2}, Scheme 1)[14,15] or between Michaelis constants (K_m) and catalytic rate constant (k_{cat})[16] can be found in the literature. Recently MOSAIC modeling has been used for dynamic optimization of the pyrimidine – purine phosphorolytic enzymatic transglycosylation.[17] This theoretical computational study is based entirely on the published kinetic parameters. However, this attempt to facilitate the optimal choice of the reaction conditions has not been experimentally verified.

In this publication, we present an original mathematical approach based on the equilibrium constants of enzymatic phosphorolysis for quantification of phosphorolytic transglycosylation at the equilibrium state when the highest content of the new target nucleoside is attained. The theory is verified by a complete set of measurements of the outcome of the transglycosylation reaction Urd + Ade ⇌ Ura + Ado (abbreviations are given according to the recommendations of the IUPAC-IUB Commission on Biochemical Nomenclature: Urd – uridine, Ade – adenine, Ura – uracil, Ado – adenosine). This methodology makes the choice of optimal reagent concentrations and their ratios routine and straightforward. It is advantageous over the widely applied trial-and-error approach and facilitates the choice of the optimal strategy for isolation of the target product and recycling of the other components.

Results and Discussion

Theoretical analysis

The overall transglycosylation process can be described as two simultaneous equilibrium reactions (Scheme 1), where K_{rB1} and K_{rB2} are equilibrium constants of corresponding phosphorolysis reactions. These constants are independent on each other and do not depend on the enzymes catalyzing phosphorolysis reactions. Therefore, there should be a mathematical relation between the equilibrium constants, starting concentrations of initial components and the equilibrium concentrations of the six species involved in this process. Our literature survey revealed a lack of such studies of equilibrium processes for this particular complex reaction.

The equations for relationship of the equilibrium concentrations can be derived from the material balance of the reaction:

$$[r]_T = [rB1] + [rP] + [rB2]$$
$$[B1]_T = [rB1] + [B1]$$
$$[B2]_T = [rB2] + [B2]$$
$$[P]_T = [rP] + [P],$$

where index T refers to the total (or initial) concentration of a component.

It is evident that $[rB1]_T = [r]_T = [B1]_T$, and it follows from the first two equations above that $[rP] = [B1] - [rB2]$. In the same manner, combining the first and third equations, we can obtain that $[rP] = [B1]_T - [B2]_T + [B2] - [rB1]$.

To ease sufficiently further notations, we denote $[B1] = x$, $[rB2] = y$, $[rB1]_T = C_{rB1}$, and $[B2]_T = C_{B2}$, $[P]_T = C_P$. Therefore, two unknown variables x and y, with assumption $[P]_T = C_P >> [rP]$, can be evaluated by solving a set of two nonlinear equations:

$$\begin{cases} \mathrm{K_{rB1}} = \dfrac{(x-y)x}{(C_{\mathrm{rB1}}-x)C_{\mathrm{P}}} \\ \mathrm{K_{rB2}} = \dfrac{(x-y)(C_{\mathrm{B2}}-y)}{yC_{\mathrm{P}}} \end{cases}$$

Omitting routine algebraic manipulations (Section S1.1 in the Supporting Information), the final equations for *x* and *y* calculations are:

$$x^3(\mathrm{K_{rB1}}-\mathrm{K_{rB2}}) - x^2\left[\mathrm{K_{rB1}}(C_{\mathrm{rB1}}+C_{\mathrm{B2}}) - \mathrm{K_{rB1}^2}C_P + \mathrm{K_{rB1}K_{rB2}}C_{\mathrm{P}}\right] + \\ + x(\mathrm{K_{rB1}}C_{\mathrm{rB1}}C_{\mathrm{B2}} - 2\mathrm{K_{rB1}^2}C_{\mathrm{B2}}C_{\mathrm{P}} + \mathrm{K_{rB1}K_{rB2}}C_{\mathrm{B2}}C_{\mathrm{P}}) + \mathrm{K_{rB1}^2}C_{\mathrm{B2}}^2C_{\mathrm{P}} = 0 \quad (1)$$

$$y = x - \mathrm{K_{rB1}}C_{\mathrm{P}}\left(\frac{C_{\mathrm{rB1}}}{x} - 1\right) \quad (2)$$

Numerical solution of cubic Equation (1) for the given equilibrium constants and initial concentrations of components yields *x*, which then is used to calculate *y* via Equation (2). Hence, we were able to calculate equilibrium concentrations of all six components (Scheme 1).

An important feature of the reaction is the invariance of the yield of products on the volume of the reaction mixture at constant ratios of initial compounds (P, rB1 and B2). I.e., the yield does not change with diluting or concentrating the whole reaction mixture. This follows from Equations (1) and (2). With diluting, the ratio of the initial concentrations C_{rB1}:C_{B2}:C_{P} remains constant, and we can rewrite it as C_{rB1}:C_{B2}:C_{P} = *C*:*mC*:*nC*. Then Equation (1) can be rewritten as follows:

$$\xi^3(\mathrm{K_{rB1}}-\mathrm{K_{rB2}}) - \xi^2\left[\mathrm{K_{rB1}}(1+m) - \mathrm{K_{rB1}^2}n + \mathrm{K_{rB1}K_{rB2}}m\right] + \\ + \xi(\mathrm{K_{rB1}}m - 2\mathrm{K_{rB1}^2}mn + \mathrm{K_{rB1}K_{rB2}}mn) + \mathrm{K_{rB1}^2}m^2n = 0$$

where $\xi = x/C$ (notice: the yield of B1 in % is equal to 100*x*/*C*). The new function $f(\xi,m,n)=0$ is independent on concentration. The same holds for the yield of nucleoside rB2:

$$y = x - \mathrm{K_{rB1}}nC\left(\frac{C}{x} - 1\right), \text{ or } \frac{y}{C} = \xi - \mathrm{K_{rB1}}n\left(\frac{1}{\xi} - 1\right)$$

(notice: the yield of rB2 in % is equal to 100*y*/*C*).

It is possible to simplify Equation (1) assuming C_{P} = 0 and C_{rB1} = C_{B2} = *C*. In this case it is transformed to the form:

$$x^2(\mathrm{K_{rB1}}-\mathrm{K_{rB2}}) - 2x\mathrm{K_{rB1}}C + \mathrm{K_{rB1}}C^2 = 0.$$

Its solution gives the only one positive result:

$$x = C\sqrt{\mathrm{K_{rB1}}/\mathrm{K_{rB2}}}\Big/\left(1+\sqrt{\mathrm{K_{rB1}}/\mathrm{K_{rB2}}}\right).$$

From Equation (2) it follows that *x* = *y*. In chemical terms, this result describes the "ideal" (direct) transglycosilation rB1 + B2 ⇌ rB2 + B1 with equilibrium constant $\mathrm{K_{eq}} = \dfrac{[\mathrm{rB2}][\mathrm{B1}]}{[\mathrm{rB1}][\mathrm{B2}]} = \dfrac{\mathrm{K_{rB1}}}{\mathrm{K_{rB2}}}$ (Section S1.2).

The yield of the products for such reactions can be calculated as follows:

$$\mathrm{yield}(\%) = 100x/C = \frac{100\sqrt{\mathrm{K_{rB1}}/\mathrm{K_{rB2}}}}{1+\sqrt{\mathrm{K_{rB1}}/\mathrm{K_{rB2}}}} \quad (3)$$

Evidently, Equation (3) gives the maximal yield, which can be attained in phosphorolytic transglycosylation with given $\mathrm{K_{rB1}}$ and $\mathrm{K_{rB2}}$. This leads to the main requirement for the choice of substrates for phosphorolytic transglycosylation: the higher the ratio $\mathrm{K_{rB1}}/\mathrm{K_{rB2}}$, the higher the outcome of the products (Figure S1). Experimentally, the extrapolation of the yield of the final products (rB2 or B1) to zero phosphate concentration can confirm its validity.

Experimental validation

We tested the described above theoretical approach on phosphorolytic transfer of ribose moiety from Urd (rB1) to Ade (B2) with formation of Ado (rB2) and Ura (B1). In brackets, the designations of compounds are given in accord with Scheme 1. The transformation is achieved with the catalysis by both uridine phosphorylase (UP, EC 2.4.2.3) and purine nucleoside phosphorylase (PNP, EC 2.4.2.1). Initial Urd is enzymatically transformed by UP into rP and Ura. Nucleic base Ade reacts with rP in the presence of PNP, furnishing new nucleoside Ado. Both reactions are reversible and characterized by equilibrium constants

$$\mathrm{K_{Urd}} = \frac{[\mathrm{rP}][\mathrm{Ura}]}{[\mathrm{Urd}][\mathrm{P}]}, \quad \mathrm{K_{Ado}} = \frac{[\mathrm{rP}][\mathrm{Ade}]}{[\mathrm{Ado}][\mathrm{P}]}$$

The reaction was studied at 37°C and pH 7.5 in buffer solutions at different phosphate concentrations. The study included measurements of concentrations of 4 components (Urd, Ura, Ade, Ado) which were determined by HPLC equipment with UV detector (Figure S2).

For chromatographic peak calibration, the reaction solution at defined substrates concentrations was analyzed by HPLC before an addition of enzyme(s). The areas under these peaks were used as references for further calculating a component concentration at equilibrium. The establishment of equilibrium was controlled by comparison with the reverse reaction (Ado + Ura) at the same initial concentrations (200 μM). The equilibrium was considered to be established when concentration of corresponding components in the direct and the reverse reactions did not differ within the experimental errors in several consecutive measurements. The time span of 8 h was usually enough to achieve the equilibrium at the enzyme concentrations applied (Table S2). One run included two direct (Urd + Ade) and one reverse (Ado + Ura) reactions (Section S4.1).

In Figure 1 we represent the experimental equilibrium concentrations (and their standard deviations) for 5 components (Urd, Ade, Ura, Ado and rP). At first we planned to use the reported values of equilibrium constants K_{Urd} and K_{Ado} for the calculation of the theoretical curves. However, brief literature search reveals extreme variations of K_{Urd} values in narrow pH and temperature intervals: 3.1×10^{-2} (pH 7.4, 37°C),[18] 1.09×10^{-3} (pH 7, 25°C),[19] 0.54 – 0.61 (pH 7.56, 30°C),[20] 0.17 (pH 7.5, 37°C).[21]

According to the theoretical considerations given above, both equilibrium constants (K_{Urd} and K_{Ado}) can be extracted from our experimental data. The calculations (Section S4.1, Table S4) give K_{Urd} = 0.153±0.014 and K_{Ado} = 0.00845±0.00085 (For comparison, we obtained following values of these constants from the phoshprolysis reactions: K_{Urd} = 0.1492±0.0035 (UP, pH 7.5, 37°C) and K_{Ado} = 0.00804±0.0020 (PNP, pH 7.5, 37°C) (Sections S5.1 and S5.2).

Based on these values, the theoretical curves (Equations (1) – (2) and the equations of material balance) were calculated (Figure 1). The accordance of experimental points with theoretical curves proves that transglycosylation is indeed governed by the equilibrium constants of phosphorolyses of the starting and final nucleosides. The experimental points for Ura and Ado tend to converge at decrease of phosphate concentration. The same tendency is observed for the pair Ade – Urd. At C_P = 0, the "ideal" yield of Ado calculated with Equation (3) is equal to

$$100\sqrt{0.139/0.0077}\Big/\left(1+\sqrt{0.139/0.0077}\right)=80.97\%$$

Noteworthy, the experimental yield of Ado at the lowest phosphate concentration (200 μM) is 79.2%, which is close to the "ideal" value.

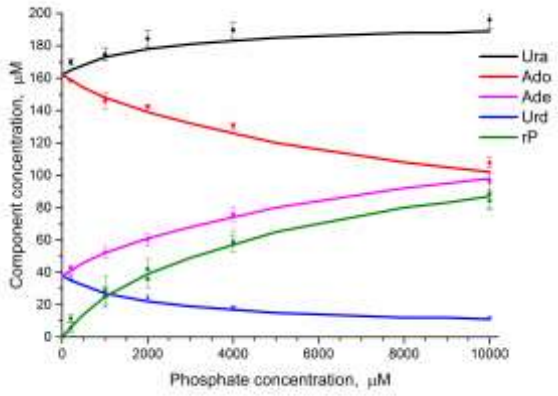

Figure 1. Equilibrium concentrations versus phosphate concentration in the reaction Urd + Ade ⇌ Ura + Ado (pH 7.5, 37°C). Colored curves – calculation with C_{Urd} = C_{Ade} = 200 μM, K_{Urd} = 0.153, K_{Ado} = 0.00845. Points – experimental data (Table S3).

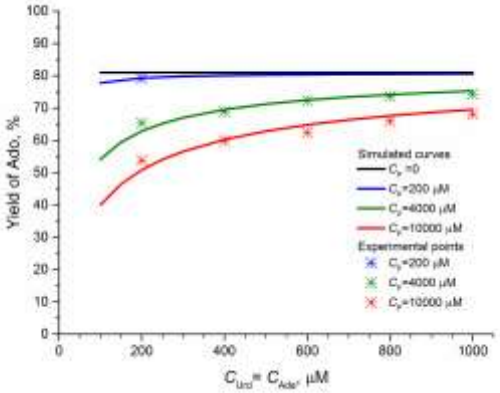

Figure 2. The effect of increasing initial concentrations of both Urd and Ade on the yield of Ado at different phosphate concentrations (pH 7.5, 37°C). Solid lines are theoretical curves with K_{Urd} = 0.153 and K_{Ade} = 0.00845; stars – experimental points (Table S6).

Using the approved algorithm, it is possible to quantify the influence of initial component concentration(s) on the outcome of the process.

Figure 1 shows that an increase of phosphate concentration results in drop of Ado yield. To minimize the negative effect of the phosphate concentration on the yield of Ado, two variants are possible. The first variant is an increase of the initial concentrations of both Urd and Ade at C_P = const. The examples for ratio Urd/Ade = 1:1 (Section S4.2) are presented in Figure 2. Increasing the initial concentrations of both compounds at constant phosphate concentration makes it possible to approach to the "ideal" yield of Ado (81 %).

The second variant is an increase of the initial concentration of one component, Urd or Ade, leaving value of C_P constant (4.3). Figure 3 illustrates that. One can see that the choice of the component (Ade or Urd) used in excess does not affect the yield of the reaction at the given K_{Urd} and K_{Ado} values. Nevertheless, these data can be applied to choose a component to be taken in excess. If the acceptor base is hardly available, it is necessary to use the excess of ribose donor to convert as much base as possible. On the other hand, when monosaccharide donor is hardly available, it is useful to take an excess of base.

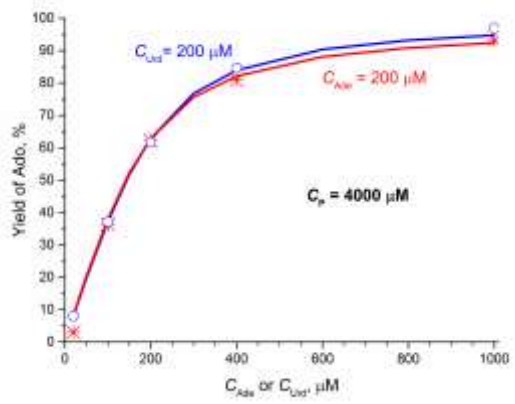

Figure 3. The yield of Ado (red) and conversion of Urd (blue) versus the initial concentration of Urd at (pH 7.5, 37°C). Solid lines are theoretical curves with K_{Urd} = 0.153, K_{Ado} = 0.00845, C_P = 4000 μM, C_{Ade} = const = 200 μM (red), and C_{Urd} = const = 200 μM (blue); stars and circles – experimental points (Tables S9 and S10).

Finally, from the set of experimental data given above (Figures 1 and 2), we can prove the validity of the mathematically drawn conclusion of invariance of Ado yield on the alteration of the volume of the whole reaction mixture. This is illustrated in Figure 4. This feature of the reaction is very important for practice, as most nucleosides and nucleic bases have limited solubility in water. Thus, it is possible to work at high dilution without any loss in the yield of the target nucleoside. This is important because the starting compounds and products can inhibit NPs at high concentrations.

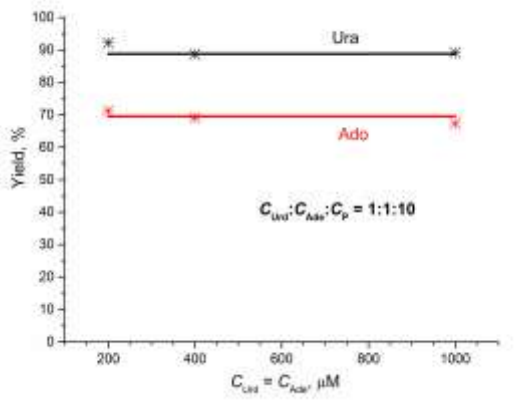

Figure 4. The invariance of the yield of Ura (black) and Ado (red) with concentrating (or diluting) the whole reaction mixture at pH 7.5, 37°C. Solid lines are theoretical curves with K_{Urd} = 0.153 and K_{Ado} = 0.00845; stars experimental points.

The experimental data validate the theoretical prediction that the equilibrium phosphorolysis constants determine the outcome of transglycosylation. This opens an alternative way for evaluation of these constants from transglycosylation runs. An advantage of this approach is a possibility to obtain simultaneously two constants from a single experimental run.

The suggested method can be applied in the cases where the reaction is carried out for particular enzymes and substrates at the equilibrium. If the equilibrium is not reached, the choice of optimal enzymes can be essential in terms of the reaction kinetics, which is analyzed in the recently published study (ref. [17]). However, for the enzymes chosen, the theory described above allows us to optimize the reaction conditions. So, both approaches can complement each other.

Summarizing the results presented in this work, we can draw several methodological conclusions for a successful practical application of transglycosylation. The equilibrium phosphorolysis constant of initial nucleoside must be as higher as possible in comparison with that of the final nucleoside. Further optimization of the yields of the desired products includes minimization of phosphate/substrate ratio, and (or) the use of one component in excess to the other. In the case of limited solubility of nucleosides and nucleic bases, it is possible to perform the process at high dilution without a loss in the yield.

Conclusion

In the present work, we have developed a theoretical approach for the quantitative prediction of phosphorolytic transglycosylation yield at equilibrium. The method is based on the fact that such outcome is governed entirely by equilibrium phosphorolysis constants of the initial and final nucleosides. These constants can usually be determined in the course of studies of the enzymatic reactions. They can also be evaluated from transglycosylation reactions and used for optimization of the process. The same algorithm might be applied for the other complex reversible reactions. For example, we can point out transfer of 5'-phosphoribosyl moiety in nucleotide chemistry, phosphorolytic transfer of monosaccharide residue in carbohydrate chemistry and some other related equilibrium processes.[7]

The proposed approach is advantageous over the traditional blind and cumbersome trial-and-error methodology for improving the product yield in complex enzymatic processes. Having once determined the equilibrium constants, one can calculate the yield of the desired product at different reagents ratios and concentration. Besides, the knowledge of all equilibrium concentrations at

transglycosylation obviously allows us to choose the optimal isolation strategy.

Experimental Section

All chemicals and solvents were of analytical grade or higher and purchased, if not stated otherwise, from Sigma–Aldrich (United States), Merck (Germany), Reakhim (Russia), and Fisher Scientific (United Kingdom).

Uridine phosphorylase from *E.coli* (91 U/ml, 2.5 mg/ml solution), **purine nucleoside phosphorylase** *E.coli* (80 U/ml, 3.99 mg/ml solution) were kindly presented by Dr R.S. Esipov from IBCH RAS and purine nucleoside phosphorylase *E.coli* (295 U/ml, 32.0 mg/ml solution) purchased from Sigma–Aldrich (United States).

Analytical HPLC was run using a Gilson Inc. (United States) HPLC system (Gilson's 2×305, 306 pumps, 811B dynamic mixer, 621 Data module and 115 UV-detector) or with an Akvilon (Russia) HPLC system (2×Stayer pumps (2nd series), a Stayer MS16 dynamic mixer and a Stayer 104M UV-Vis detector). The analysis were performed on 4.6×150mm column (5µm, Luna® C_{18}(2) 100 Å, Part No 00F-4252-EC, Phenomenex (United States)) equipped with EC security guard (4.0×3 мм, 5 µm, C_{18} Part No AJ0-4287, Phenomenex (United States)) or on 4×150mm Dr. Maisch HPLC column (5µm, Reprosil-Pur C_{18}-AQ 120 Å, Part No r15.aq.s1504, Dr. Maisch HPLC GmbH (Germany) in a linear acetonitrile gradient in deionized water. The conditioning and equilibration of the chromatographic column was conducted for at least half an hour after each measurement.

For preparation of all solutions water was purified using Milli-Q® water ultrafiltration station (Merck Millipore, United States). The pH values were determined with a microprocessor-based pH (mV- C) bench meter 211 (Hanna Instruments, Germany), equipped with an HI1131B double junction combination pH electrode and an HI7662 stainless steel temperature sensor for pH compensation.

For the preparation of the sample solutions a high quality LAB MATE instrument with HTL tips was used.

General transglycosylation protocol. To a sample solution (1 mL, see Table S1) there were added 2 µL of 2.50 mg/ml solution of UP *E. coli* (0.182 U) and 3 µL of 3.99 mg/ml solution of PNP *E. coli* (0.24 U). The reaction mixture was incubated at 37ºC, and was monitored by HPLC. The equilibrium was considered to be established when concentration of components in the direct and the reverse reactions were similar. For the solutions with C_{Urd}:C_{Ade}:C_P = 1:1:1 and C_{Ado}:C_{Ura}:C_P = 1:1:1 this required 8 h. This time span was taken for all other reactions at the same enzyme(s) loadings. The experimental data for the direct and the reverse transglycosylation reactions are summarized in Table S2 (the values labelled by italic are authentic concentrations which were used for calibration of HPLC peaks).

The HPLC data at t = 0 was used for calibration coefficients (α) calculations. The following average values were obtained: α_{Ura} = 0.1473±0.0018, α_{Urd} = 0.1137±0.0023, α_{Ade} = 0.08973±0.0032, α_{Ado} = 0.07794±0.0013 (dimension µM/mVsec, standard deviations σ_n are given). Using these values, the equilibrium concentrations were calculated, and the data are presented in Table S2. Average values of equilibrium concentrations are given in Table S3.

Direct determination of phosphorolysis constants

Determination of K_{Urd} by phosphorolysis of Urd catalyzed with UP from *E. coli*. The sample solutions (1 mL) were prepared in a manner described above. The phosphorolysis reaction was initiated by addition of 2 µL of 2.50 mg/ml solution of UP *E. coli* (0.182 U). The reaction was incubated at 37ºC and monitored by HPLC. Time span of 8 h was enough for the establishment of equilibrium. The results are collected in Table S11. The constant was calculated according to formula

$$K_{Urd} = \frac{(C_{Urd} - [Urd])^2}{[Urd](C_P - C_{Urd} + [Urd])}$$

Determination of K_{Ado} by phosphorolysis of Ado catalyzed with PNP from *E. coli*. The same approach as presented above was used. The phosphorolysis of Ado was triggered by addition of 3 µL of 3.99 mg/ml solution of PNP *E. coli* (0.24 U). The reaction was incubated at 37ºC and monitored by HPLC. Time span of 8 h was enough for the establishment of equilibrium. The results are collected in Table S12. The constant was calculated according to formula

$$K_{Ado} = \frac{(C_{Ado} - [Ado])^2}{[Ado](C_P - C_{Ado} + [Ado])}$$

Acknowledgements

This work was supported by the Russian Science Foundation (project No. 16-14-00178)

References

[1] a) L. P. Jordheim, D. Durantel, F. Zoulim, C. Dumontet, *Nat. Rev. Drug Discovery* **2013**, *12*, 447–464; b) L. E. Iglesias, E. S. Lewkowicz, R. Medici, P. Bianchi, A. M. Iribarren, *Biotechnol. Adv.* **2015**, *33*, 412–434; c) E. De Clercq, G. Li, *Clinical Microbiol. Rev.* **2016**, *29*, 695–747; d) M. J. Lapponi, C. W. Rivero, M. A. Zinni, C. N. Britos, J. A. Trelles, *J. Mol. Catal. B: Enzymatic* **2016**, *133*, 218–233.

[2] G. Niu, H. Tan, *Trends Microbiol.* **2015**, *23*, 110–119.

[3] a) L. Bodei, A. I. Kassis, S. J. Adelstein, G. Mariani, *Cancer Biother. Radiopharm.* **2003**, *18*, 861–877; b) R. Alberto, H. P. N'Dongo, M. Clericuzio, S. Bonetti, E. Gabano, C. Cassino, M. Ravera, D. Osella, *Inorg. Chim. Acta* **2009**, *362*, 4785–4790.

[4] V. I Tararov, A. Tijsma, S. V Kolyachkina, V. E Oslovsky, J. Neyts, M. S Drenichev, P. Leyssen, S. N. Mikhailov, *Eur. J. Med. Chem*. **2015**, *90*, 406–413.

[5] J. Boryski, *Curr. Org. Chem*. **2008**, *12*, 309–325.

[6] E. S. Lewkowicz, A. M. Iribarren, *Curr. Org. Chem* **2006**, *10*, 1197–1215.

[7] a) R. N. Goldberg, Y. B. Tewari, *J. Phys. Chem. Ref. Data* **1994**, *23*, 547–617; b) R. N. Goldberg, Y. B. Tewari, T. N. Bhat, *J. Phys. Chem. Ref. Data* **2007**, *36*, 1347–1397.

[8] a) M. I. Kharitonova, A. O. Denisova, V. L. Andronova, A. L. Kayushin, I. D. Konstantinova, S. K. Kotovskaya, G. A. Galegov, V. N. Charushin, A. I. Miroshnikov, *Bioorg. Med. Chem. Letters* **2017**, *27*, 2484–2487; b) G. Cattaneo, M. Rabuffetti, G. Speranza, T. Kupfer, B. Peters, G. Massolini, D. Ubiali, E. Calleri, *ChemCatChem*. **2017**, *9*, 4614–4620; c) S. P. Ozcáriz, *EC Microbiology* **2017**, *6*,

35–38; d) H. Yehia, S. Kamel, K. Paulick, P. Neubauer, A. Wagner, *Cur. Pharm. Design* **2017**, *23*, 6913–6935.

[9] I. A. Mikhailopulo , A. I. Zinchenko , Z. Kazimierczuk, V. N. Barai , S. B. Bokut, E. N. Kalinichenko, *Nucleosides & Nucleotides* **1993**, *12*, 417–422.

[10] I. Serra, T. Bavaro, D. A. Cecchini, S. Daly, A. M. Albertini, M. Terreni, D. Ubiali *J. Mol. Catal. B: Enzymatic* **2013**, *95*, 16–22.

[11] G. L. Cote, B. Y. Tao, *Glycoconjugate Journal* **1990**, *7*, 145–162.

[12] A. Fresco-Taboada, I. de la Mata, M. Arroyo, J. Fernández-Lucas, *Appl. Microbiol. Biotechnol.* **2013**, *97*, 3773–3785.

[13] Y. Mitsukawa, M. Hibi, N. Matsutani, N. Horinouchi, S. Takahashi, J. Ogawa, *J. Biosci. Bioeng.* **2017**, *123*, 659–664.

[14] I. A. Mikhailopulo, A. I. Miroshnikov, *Mendeleev Commun*. **2011**, *21*, 57–68.

[15] M. S. Drenichev, C. S. Alexeev, N. N. Kurochkin, S. N. Mikhailov, *Adv. Synth. Catal*. **2018**, *360*, 305–312.

[16] X. Zhou, K. Szeker, L.-Y. Jiao, M. Oestreich, I. A. Mikhailopulo, P. Neubauer, *Adv. Synth. Catal*. **2015**, *357*, 1237–1244.

[17] T. Wilms, D. F. Rischawy, T. Barz, E. Esche, J.-U. Repke, A. Wagner, P. Neubauer, M. N. C. Bournazou, *Chemie Ingenieur Technik* **2017**, *89*, 1523–1533.

[18] R. Bose, E. W. Yamada, *Biochemistry* **1974**, *13*, 2051–2056.

[19] R. A. Alberty, *Biophys. Chem.* **2007**, *127*, 91–96.

[20] A. Vita, C. Y. Huang, G. Magni, *Arch. Biochem. Biophys.* **1983**, *226*, 687–692.

[21] N. G. Panova, E. V. Shcheveleva, C. S. Alexeev, V. G. Mukhortov, A. N. Zuev, S. N. Mikhailov, R. S. Esipov, D. V. Chuvikovsky, A. I. Miroshnikov, *Molecular Biology* (Russia) **2004**, *38*, 770–776.

10.1002/adsc.201800411

FULL PAPER

Quantitative Prediction of Yield in Transglycosylation Reaction Catalyzed by Nucleoside Phosphorylases

Adv. Synth. Catal. **Year**, *Volume*, Page – Page

Cyril S. Alexeev, Irina V. Kulikova, Sergei Gavryushov, Vitali I. Tararov, Sergey N. Mikhailov*

TOC Graphic

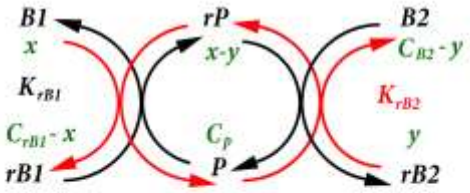

$$x^3(K_{rB1}-K_{rB2})-x^2[K_{rB1}(C_{rB1}+C_{B2})-K_{rB1}^2C_p+$$
$$+K_{rB1}K_{rB2}C_p]+x(K_{rB1}C_{rB1}C_{B2}-2K_{rB1}^2C_{B2}C_P+$$
$$+K_{rB1}K_{rB2}C_{B2}C_p)+K_{rB1}^2C_{B2}^2C_p=0$$

$$y=x-K_{rB1}C_p[\frac{C_{rB1}}{x}-1]$$